La0.7Sr0.3MnO3 suspended microbridges for uncooled bolometers made using reactive ion etching of the silicon substrates

Shuang Liu, Bruno Guillet, Ammar Aryan, Carlo Adamo, Cédric Fur, Jean-Marc Routoure, Florian Lemarié, D.G. Schlom, Laurence Mechin

▶ **To cite this version:**

Shuang Liu, Bruno Guillet, Ammar Aryan, Carlo Adamo, Cédric Fur, et al.. La0.7Sr0.3MnO3 suspended microbridges for uncooled bolometers made using reactive ion etching of the silicon substrates. MNE2012 (38th International Micro & Nano Engineering Conference), Sep 2012, Toulouse, France. 111, pp.101-104, 2013. <hal-00977471>

HAL Id: hal-00977471

https://hal.archives-ouvertes.fr/hal-00977471

Submitted on 11 Apr 2014

HAL is a multi-disciplinary open access archive for the deposit and dissemination of scientific research documents, whether they are published or not. The documents may come from teaching and research institutions in France or abroad, or from public or private research centers.

L'archive ouverte pluridisciplinaire **HAL**, est destinée au dépôt et à la diffusion de documents scientifiques de niveau recherche, publiés ou non, émanant des établissements d'enseignement et de recherche français ou étrangers, des laboratoires publics ou privés.

$La_{0.7}Sr_{0.3}MnO_3$ suspended microbridges for uncooled bolometers made using reactive ion etching of the silicon substrates

S. Liu [a], B. Guillet [a], A. Aryan [a], C. Adamo [b], C. Fur [a], J.-M. Routoure [a], F. Lemarié [c], D.G. Schlom [b,d], L. Méchin [a,*]

[a] GREYC, UMR 6072, CNRS-ENSICAEN-Université de Caen Basse Normandie, 6 Bd Maréchal Juin, Caen 14050, France
[b] Department of Materials Science and Engineering, Cornell University Ithaca, NY 14853-1501, USA
[c] CIMAP, UMR 6252, CNRS-CEA-ENSICAEN-Université de Caen Basse-Normandie, 6 Bd Maréchal Juin, Caen 14050, France
[d] Kavli Institute at Cornell for Nanoscale Science, Ithaca, NY 14853, USA

A B S T R A C T

Suspended $La_{0.7}Sr_{0.3}MnO_3$ (LSMO) microbridges were fabricated using standard silicon micromachining techniques. First epitaxial LSMO thin films were deposited on $SrTiO_3$ (STO) buffered Si (001) substrates by molecular-beam epitaxy. A simple two photolithography step process using the reactive ion etching of the silicon substrate to release the suspended microbridges was developed. The electrical resistivity as a function of temperature of 4 µm wide 50–200 µm long and 75 nm thick LSMO/STO fully processed suspended microbridges was very close to the characteristics of the initial LSMO thin films, demonstrating that the fabrication process did not degrade the quality of the LSMO. The thermal conductance of the processed bolometers was very low (of the order of 10^{-7} W K^{-1}) at 300 K. These structures are promising for uncooled bolometer applications and other micro-electromechanical systems based on LSMO or other epitaxial functional oxides.

Keywords:
Epitaxial oxide
Silicon
Micromachining
Bolometers
Manganites
Molecular beam epitaxy

1. Introduction

Thanks to the large resistance change at the metal-to-insulator (M-I) transition and high spin polarization, the manganite composition $La_{0.7}Sr_{0.3}MnO_3$ (LSMO) is a promising candidate for a new generation of sensors operated at room temperature including bolometers and magnetic sensors [1–4]. A bolometer is a thermal detector, i.e., the absorbed incoming radiation induces a temperature rise of the active area. In order to increase the bolometer sensitivity, one has to reduce the thermal conductance between the active area and the substrate in order to increase the temperature rise, and also choose a material with a large variation of resistance with temperature. The latter variation is named the temperature coefficient of resistance TCR = $(1/R) \times (dR/dT)$. TCR values in LSMO are about 2% K^{-1} at temperatures close to 300 K [5], which is about one order of magnitude better that platinum (with TCR of 0.385% K^{-1}) [6]. Reduction of thermal conductance can be achieved by removing the substrate below the LSMO film. Since the heated volume is reduced, the thermal response time of such suspended bolometers can be small. Our free-standing $La_{0.7}Sr_{0.3}MnO_3/SrTiO_3$ structures are therefore promising for sensitive and fast uncooled bolometers.

Functional oxide thin films such as manganites are commonly grown on single crystalline oxide substrates with lattice parameters matching as closely as possible those of the film material [7]. This is because the resulting epitaxial LSMO films have much higher TCR values and lower noise than polycrystalline LSMO films. In view of applications, and in particular, of microelectromechanical systems (MEMS) fabrication, the epitaxial integration of LSMO with silicon substrates is a huge advantage because of their compatibility with standard microelectronics processes and existing micromachining techniques. The growth of epitaxial oxide thin films on silicon substrates is, however, challenging because if the silicon substrate is oxidized before a crystalline oxide is nucleated on top of it, the crystalline template needed for epitaxy can be lost. Different solutions using various epitaxial buffer layers have been proposed [8–13].

There are rather few studies of epitaxial manganites-based MEMS. Pellegrino et al. [14] reported the fabrication and modeling of MEMS entirely made of crystalline oxides. No silicon substrates were used. Using $SrTiO_3$ (STO) substrates and chemical etching of a sacrificial layer, they fabricated suspended STO (001) microcantilevers prior to the deposition of the epitaxial LSMO layers. These suspended heterostructures could be used for the realization of devices making use of strain effect in the overgrown of a LSMO film coherently strained to the underlying STO substrate. Kim and Grishin [15] demonstrated the feasibility of the fabrication of free-

* Corresponding author. Tel.: +33 231452692; fax: +33 231452698.
E-mail address: laurence.mechin@ensicaen.fr (L. Méchin).

standing epitaxial $La_{1-x}(Sr,Ca)_xMnO_3$ (LSCMO) membranes on Si using a combination of Ar ion beam etching and inductively coupled SF_6 and C_4F_8 plasma-etching processes. The electrical transport properties of the 50 nm thick LSCMO films deposited on $Bi_4Ti_3O_{12}/CeO_2$/YSZ on silicon were, however, significantly degraded after the micromachining process. The electrical resistivity after processing was increased 7 times compared to the starting film.

In this paper we demonstrate the fabrication of epitaxial LSMO/STO suspended microbridges using ion etching followed by reactive ion etching (RIE) of the silicon substrate underlying the LSMO/STO, without degrading the electrical properties of LSMO. The fabrication process is described in Section 2. In Section 3, we present the electrical resistivity versus temperature characteristics of the suspended LSMO/STO microbridges. Section 4 reports thermal conductance measurements.

2. Fabrication process

We chose STO, a perovskite with a cubic unit cell of 0.3905 nm, as the buffer layer for the growth of our epitaxial LSMO thin films on silicon. Significant progress has been made in the controlled growth of epitaxial oxide thin films on silicon [16]. In particular the pionneering work of McKee et al. [17] demonstrated the epitaxial growth of high quality STO on Si (001) substrates by molecular-beam epitaxy (MBE). In our case 75 nm thick LSMO films were grown on 20 nm thick STO buffer layers on Si (001) substrates by reactive MBE [18]. A substrate temperature of 670 °C and an ozone background pressure of 3×10^{-7} Torr were used for the growth of the LSMO [19]. The X-ray diffraction (XRD) in Fig. 1 shows that both LSMO and STO layers are fully (001) oriented and of high epitaxial quality. θ–2θ scans also reveal that both the STO and the LSMO out-of-plane lattice parameters (0.3890 nm and 0.3850 nm, respectively) are slightly reduced compared to bulk values (0.3905 nm and 0.3880 nm, for bulk STO and LSMO, respectively), thus revealing an in-plane tensile strain in the films. The inset shows the XRD rocking curves in the ω-scan configuration around the STO 002 and LSMO 002 peaks. The full width at half maximum values are 0.22° and 0.18°, for STO and LSMO, respectively. A detailed study of the structural, electrical and magnetic properties of these films is reported in [13].

The fabrication process of the free-standing LSMO/STO bridges is shown in Fig. 2a. It is very simple since it needs only two photolithographic steps [20]. After LSMO and STO deposition, contact

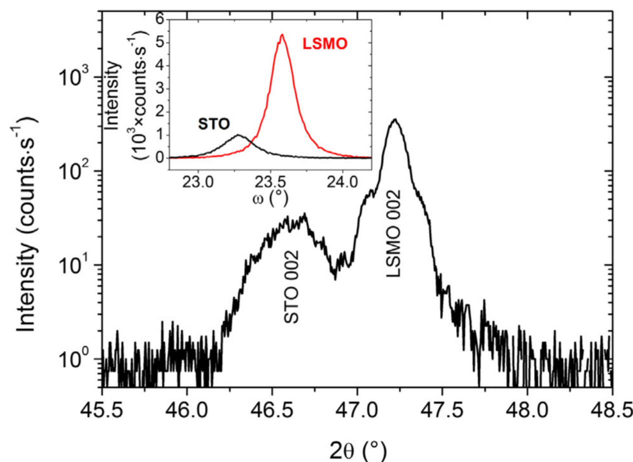

Fig. 1. X-ray diffraction patterns in the θ–2θ configuration of the 75 nm thick LSMO films on STO/Si. The inset shows the rocking curves measured in the ω-scan configuration around the STO 002 and LSMO 002 peaks.

pads were defined by standard UV photolithography and chemical etching. A 200 nm thick gold layer was deposited by ion gun deposition and the sample was annealed at 400 °C in an O_2 pressure of 400 mbar for 60 min in order to reduce the contact resistance (step I in Fig. 2a). The bridge geometry was defined by standard UV photolithography, followed by Ar ion beam milling down to the silicon substrate as shown in step II of Fig. 2a. The photoresist was not removed. RIE in SF_6 gas (0.05 mbar; 30 sccm) at a power of 30 W was applied from the front side in order to etch the silicon under what would become suspended microbridges. These conditions were chosen in order to enhance the isotropic nature of the process, i.e., high-pressure atmosphere and low power. Silicon is etched vertically at 0.5 μm min^{-1} and laterally at 0.7 μm min^{-1} and the 4 μm wide LSMO/STO bridges remain free-standing (step III in Fig. 2a). An optical micrograph of the four 4 μm wide LSMO/STO suspended microbridges is shown in Fig. 2c. 200 μm, 150 μm, 100 μm and 50 μm long bridges were successfully fabricated. A tilted scanning electron micrograph (SEM) of the 100 μm long suspended microbridges is displayed in Fig. 2b. In the SEM photograph the white areas are suspended LSMO/STO layers.

3. Electrical characterisation

The electrical resistivity of the LSMO suspended microbridges as well as of a 600 μm wide 3 mm long non suspended LSMO line patterned on the same Si substrate were measured as a function of temperature in a four probe configuration. We used a prober with a variable temperature stage (LAKESHORE TTP4) to heat the sample up to around 360 K in a primary vacuum atmosphere, and we used a Semiconductor Parametric Analyzer (HP3562A) to plot the current–voltage $I(V)$ characteristics. Because of their high thermal isolation, the LSMO suspended structures are extremely sensitive to thermal runaway and particular attention must be paid to avoid any damage during measurements. To ensure no degradation of our suspended structures, the maximum value of the bias current during electrical resistivity measurements was limited to 5 μA. The electrical resistivity values were deduced from the slope of the I–V characteristics after having checked the linear nature of the curves (i.e., an ohmic behavior). Fig. 3 shows the electrical resistivity versus temperature characteristics of the four suspended bridges as well as of the non suspended line. The electrical resistivity at 295 K of the non suspended line is about 3.6×10^{-5} Ω m, which is close to bulk value of LSMO [21]. Interestingly the electrical resistivity at 295 K of the suspended microbridges varies in the 2.5×10^{-5}–3.1×10^{-5} Ω m range, with decreasing electrical resistivity with increasing suspended line length. These reduced electrical resistivity values in the suspended bridges compared to the unsuspended one could be attributed to strain effects, since electrical properties of LSMO are very sensitive to strain, as in other metals in which electron–lattice interactions play a key role [19,22,23]. No direct measurements of strain in our suspended microbridges were made. We therefore cannot quantitatively correlate the measured electrical resistivity with strain, but only observe a small variation of electrical resistivity with line length. Overall the electrical resistivity values measured on suspended microbridges are of the order of the one measured on the unsuspended line.

Values of the maximum of TCR vary from 0.012 K^{-1} to 0.021 K^{-1} for the 200 μm long and the 50 μm long microbridges, respectively. These values are slightly decreased compared to the maximum value of TCR of the non suspended line (0.025 K^{-1}). The temperature of the maximum of TCR (T_{max}) is in the 305–310 K range for all the suspended microbridges and the non suspended line. These results demonstrate that our fabrication process did not degrade the LSMO

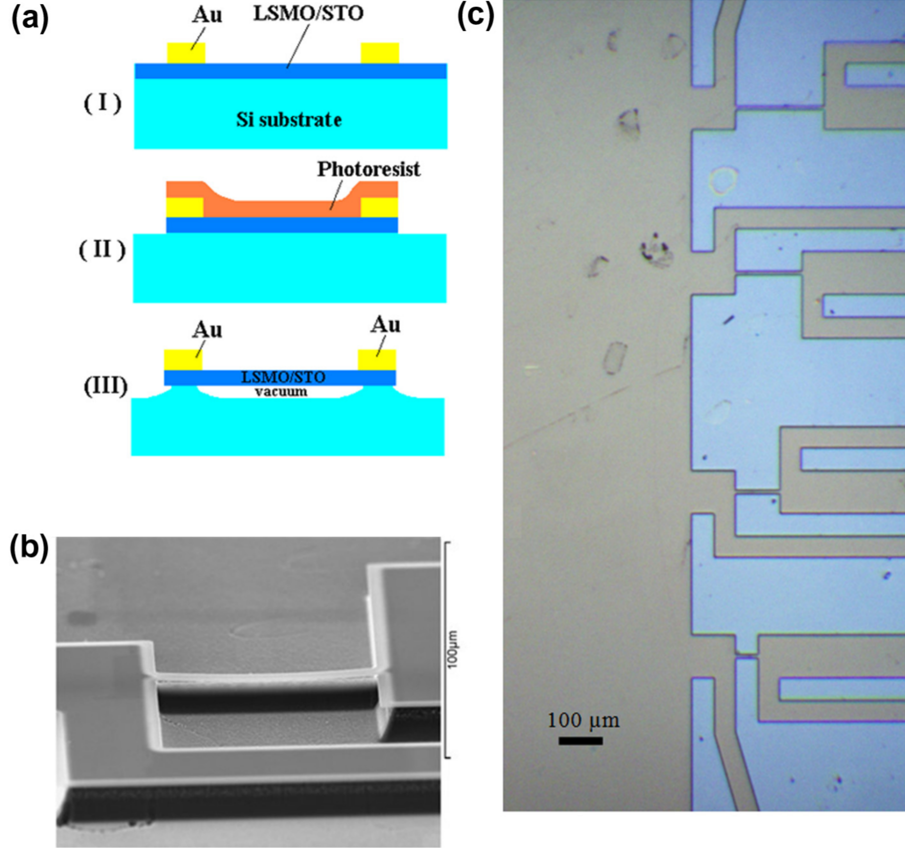

Fig. 2. (a) Fabrication steps of the suspended LSMO/STO microbridges: (I) Gold deposition and patterning for the electrical contacts; (II) Standard UV photolithography followed by Ar ion beam milling down to the silicon substrate, in order to define the device geometry, (III) RIE of silicon in SF_6, (b) SEM view of the 100 µm long LSMO suspended microbridge (white areas are suspended layers): (c) Optical micrograph of the four 4 µm wide suspended microbridges.

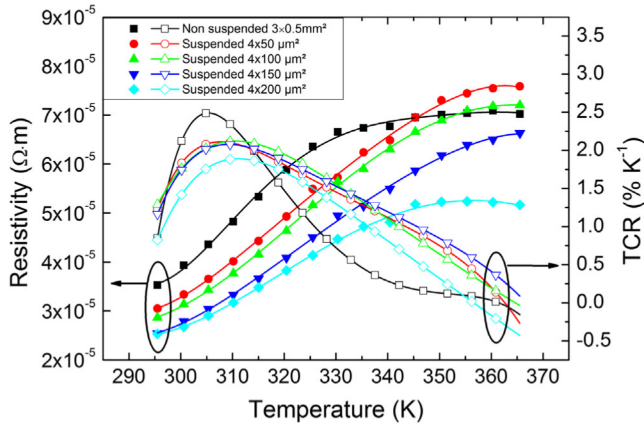

Fig. 3. Electrical resistivity (left y axis) and TCR (right y axis) versus temperature of LSMO/STO self-supported microbridges and of a non suspended LSMO line.

electrical properties. The suspended microbridges keep sufficiently good TCR values for their use in room-temperature bolometers.

4. Electrothermal characterization

The thermal conductance between the heated part of the bolometer (here the LSMO/STO self-supported bridge) and the heat sink (here the Si substrate) is an important parameter for the optimization and assessment of potential bolometers. The smaller the thermal conductance is, the higher the bolometer responsivity will be. In the following measurements the devices were placed in vacuum (at a residual pressure of about 10^{-4} mbar) so that there is no thermal conduction through the surrounding gas (i.e., no convection). The total thermal conductance can be calculated as the thermal conductance through the mechanical support only, which is the LSMO/STO self-supported microbridge itself. In the case of uniform heat production P, we can define the average temperature rise ΔT and we can show from the equation of heat flow in solids, that the thermal conductance is [20]:

$$G = \frac{P}{\Delta T} = \frac{12w}{l} \times \sum_i k_i t_i \tag{1}$$

where l and w are the length and the width of the suspended bridge, t_i and k_i are the thickness and the thermal conductivity of each layer constituting the suspended bridge, and P is the overall power received by the bridge of electrical resistance R. Calculated values of G using Eq. (1) and thermal conductivity values of LSMO and STO (2.5 and 11.6 $\mathrm{W\,m^{-1}\,K^{-1}}$, respectively [24–27]) vary from $5 \times 10^{-7}\ \mathrm{W\,K^{-1}}$ to $10^{-7}\ \mathrm{W\,K^{-1}}$ for the 50 µm and the 200 µm long suspended microbridges, respectively . We used the $\rho(T)$ curves of Fig. 3 and $I(V)$ curves in order to plot P ($P = R \times I^2$) versus T curves. Using self heating effects, the thermal conductance G values were finally determined as the slope of the $P(T)$ curves at their origin. The measured values of G at about 310 K (near $T_{\max}$) can be directly compared to calculated values at 300 K. One can see in Fig. 4 that the measured G values are very close to the calculated ones using Eq. (1). This enables us to use Eq. (1) with confidence for the future optimisation of the design of uncooled bolometers. The measured G

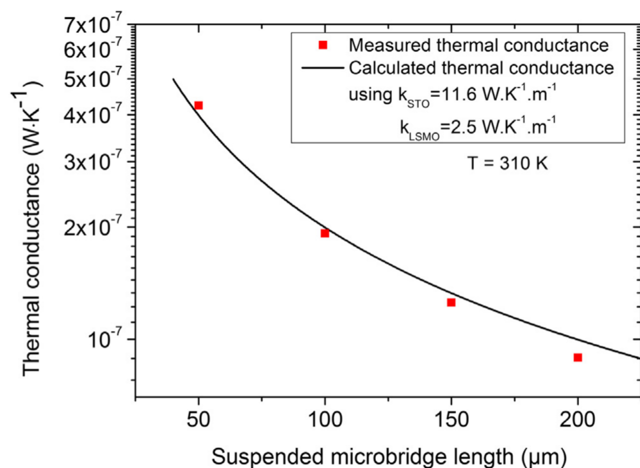

Fig. 4. Thermal conductance of 4 μm wide suspended LSMO microbridges versus microbridge length at 310 K.

values of suspended bridges have to be compared to the G values measured in non suspended bridges, which are of the order of 10^{-3} W K^{-1} (heat dissipation through the substrate). We therefore achieved a reduction by about a factor of 10^4 in the thermal conductance by removing the thermal contact between the LSMO and underlying substrate by fabricating suspended microbridges.

5. Conclusion

We successfully fabricated 4 μm wide LSMO/STO self-supported microbridges of length 50–200 μm using Ar ion milling followed by RIE of the silicon substrate. The fabrication process did not degrade the electrical properties of the LSMO film. At room temperature the measured thermal conductance was very close to calculated values and varied from $(1–5) \times 10^{-7}$ W K^{-1} for the 50 μm and the 200 μm long suspended microbridges, respectively. We have thus demonstrated that MEMS technology can be successfully applied to LSMO epitaxial functional oxides. By suspending the microbridges, we reduced the thermal conductance by a factor of 10^4, without degrading the TCR of the LSMO layer. These two achievements demonstrate that suspended LSMO microbridges are very promising for the fabrication of high sensitivity uncooled bolometers [28].

Acknowledgements

The work at Cornell was supported by AFOSR through award No. FA9550-10-1-0524.

References

[1] L. Méchin, J.M. Routoure, B. Guillet, F. Yang, S. Flament, D. Robbes, R.A. Chakalov, Appl. Phys. Lett. 87 (2005) 204103.
[2] F. Yang, L. Méchin, J.M. Routoure, B. Guillet, R.A. Chakalov, J. Appl. Phys. 99 (2006) 024903.
[3] M. Bibes, A. Barthelemy, IEEE Trans. Electron Devices 54 (2007) 1003.
[4] D. Fadil, S. Wu, P. Perna, B. Renault, M. Saïb, S. Lebargy, J. Gasnier, B. Guillet, J.-M. Routoure, S. Flament, L. Méchin, J. Appl. Phys. 112 (2012) 013906.
[5] A. Goyal, M. Rajeswari, R. Shreekala, S.E. Lofland, S.M. Bhagat, T. Boettcher, C. Kwon, R. Ramesh, T. Venkatesan, Appl. Phys. Lett. 71 (1997) 2535.
[6] P.R.N. Childs, J.R. Greenwood, C.A. Long, Rev. Sci. Instrum. 71 (8) (2000) 2959.
[7] H.U. Habermeier, J. Electroceram. 13 (2004) 23.
[8] Z. Trajanovic, C. Kwon, M.C. Robson, K.-C. Kim, M. Rajeswari, R. Ramesh, T. Venkatesan, S.E. Lofland, S.M. Bhagat, D. Fork, Appl. Phys. Lett. 69 (1996) 1005.
[9] I. Bergenti, V. Dediu, E. Arisi, M. Cavallini, F. Biscarini, C. Taliani, M.P. de Jong, C.L. Dennis, J.F. Gregg, M. Solzi, M. Natali, J. Magn. Magn. Mater. 312 (2007) 453.
[10] A.K. Pradhan, S. Mohanty, K. Zhang, J.B. Dadson, E.M. Jackson, D. Hunter, R.R. Rakhimov, G.B. Loutts, Appl. Phys. Lett. 86 (2005) 012503.
[11] A.K. Pradhan, D. Hunter, T. Williams, B. Lasley-Hunter, R. Bah, H. Mustafa, R. Rakhimov, J. Zhang, D.J. Sellmyer, E.E. Carpenter, D.R. Sahu, J.-L. Huang, J. Appl. Phys. 103 (2008) 023914.
[12] P. Perna, L. Méchin, M.P. Chauvat, P. Ruterana, Ch. Simon, U. Scotti di Uccio, J. Phys. Condens. Matter 21 (2009) 306005.
[13] L. Méchin, C. Adamo, S. Wu, B. Guillet, S. Lebargy, C. Fur, J.-M. Routoure, S. Mercone, M. Belmeguenai, D.G. Schlom, Phys. Status Solidi A 209 (2012) 1090.
[14] L. Pellegrino, M. Biasotti, E. Bellingeri, C. Bernini, A.S. Siri, D. Marré, Adv. Mater. 21 (2009) 2377.
[15] J.-H. Kim, A.M. Grishin, Appl. Phys. Lett. 87 (2005) 033502.
[16] J.W. Reiner, A.M. Kolpak, Y. Segal, K.F. Garrity, S. Ismail-Beigi, C.H. Ahn, F.J. Walker, Adv. Mater. 22 (2010) 2919.
[17] R.A. McKee, F.J. Walker, M.F. Chisholm, Phys. Rev. Lett. 81 (1998) 3014.
[18] M.P. Warusawithana, C. Cen, C.R. Sleasman, J.C. Woicik, Y. Li, L.F. Kourkoutis, J.A. Klug, H. Li, P. Ryan, L.-P. Wang, M. Bedzyk, D.A. Muller, L.-Q. Chen, J. Levy, D.G. Schlom, Science 324 (2009) 367.
[19] C. Adamo, X. Ke, H.Q. Wang, H.L. Xin, T. Heeg, M.E. Hawley, W. Zander, J. Schubert, P. Schiffer, D.A. Muller, L. Maritato, D.G. Schlom, Appl. Phys. Lett. 95 (2009) 112504.
[20] L. Méchin, J.-C. Villégier, D. Bloyet, J. Appl. Phys. 81 (1997) 7039.
[21] A. Urushibara, Y. Moritomo, T. Arima, A. Asamitsu, G. Kido, Y. Tokura, Phys. Rev. B 51 (1995) 14103.
[22] A.J. Millis, Nature 392 (1998) 147.
[23] C. Thiele, K. Dörr, S. Fähler, L. Schultz, D.C. Meyer, A.A. Levin, P. Paufler, Appl. Phys. Lett. 87 (2005) 262502.
[24] L.M. Wang, J.-H. Lai, J.-I. Wu, J. Appl. Phys. 102 (2007) 023915.
[25] I. El-Kassab, A.M. Ahmed, P. Mandal, K. Barner, A. Kattwinkel, U. Sondermann, Physica B 305 (2001) 233.
[26] H. Muta, K. Kurosaki, S. Yamanaka, J. Alloys Compd. 392 (2005) 306.
[27] D.-W. Oh, J. Ravichandran, C.W. Liang, W. Siemons, B. Jalan, C.M. Brooks, M. Huijben, D.G. Schlom, S. Stemmer, L.W. Martin, A. Majumdar, R. Ramesh, D.G. Cahill, Appl. Phys. Lett. 98 (2011) 221904.
[28] F. Niklaus, C. Vieider, H. Jakobsen, Proc. SPIE 6836 (2007) 68360D.